Nonequilibrium relaxations within the ground-state manifold in the antiferromagnetic Ising model on a triangular lattice

Eunhye Kim,[1,*] Sung Jong Lee,[2] and Bongsoo Kim[1]
[1]*Department of Physics, Changwon National University, Changwon 641-773, Korea*
[2]*Department of Physics, The University of Suwon, Hwaseong-Si, 445-743, Korea, and School of Computational Sciences, Korea Institute for Advanced Study, Seoul 130-722, Korea*

(Received 28 April 2006; revised manuscript received 17 November 2006; published 8 February 2007)

We present an extensive Monte Carlo simulation study on the nonequilibrium kinetics of triangular antiferromagnetic Ising model within the ground state ensemble which consists of sectors, each of which is characterized by a unique value of the string density p through a dimer covering method. Building upon our recent work [Phys. Rev. E **68**, 066127 (2003)] where we considered the nonequilibrium relaxation observed within the dominant sector with $p=2/3$, we here focus on the nonequilibrium kinetics within the minor sectors with $p<2/3$. The initial configurations are chosen as those in which the strings are straight and evenly distributed. In the minor sectors, we observe a characteristic spatial anisotropy in both equilibrium and nonequilibrium spatial correlations. We observe emergence of a critical relaxation region (in the spatial and temporal domain) which grows as p deviates from $p=2/3$. Spatial anisotropy appears in the equilibrium spatial correlation with the characteristic length scale $\xi_{e,V}(p)$ diverging with vanishing string density as $\xi_{e,V}(p)\sim p^{-2}$ along the vertical direction, while along the horizontal direction the spatial length scale diverges as $\xi_{e,H}\sim p^{-1}$. Analytic forms for the anisotropic equilibrium correlation functions are given. We also find that the spin autocorrelation function $A(t)$ shows a simple scaling behavior $A(t)=\mathcal{A}(t/\tau_A(p))$, where the time scale $\tau_A(p)$ shows a power-law divergence with vanishing p as $\tau_A(p)\sim p^{-\phi}$ with $\phi\simeq 4$. These features can be understood in terms of random walk nature of the fluctuations of the strings within the typical separation between neighboring strings.

DOI: 10.1103/PhysRevE.75.021106 PACS number(s): 05.50.+q, 05.70.Jk, 05.10.Ln

I. INTRODUCTION

The antiferromagnetic Ising (AFI) model on a triangular lattice is an archetypical frustrated spin system [1]. The Hamiltonian of the AFI model on a triangular lattice in two dimensions is given by

$$H = J\sum_{\langle ij\rangle} \sigma_i\sigma_j, \tag{1}$$

where $\sigma_i=\pm 1$ is the Ising spin at site i, $J>0$ the interaction strength, and $\langle ij\rangle$ denotes nearest neighbor (NN) pairs. Throughout the paper we set $J=1$. The system is frustrated since the three bonds in every elementary triangle (plaquette) cannot simultaneously satisfy the AF interaction. This geometry-induced frustration leads to an exponentially large number of ground state degeneracies, rendering nonzero entropy density at zero temperature [2,3]. Therefore no genuine long-range order exists even at zero temperature. However, it is remarkable that the ground state exhibits a critical phase in which the equilibrium spin correlation function decays algebraically with distance r as $C_e(r)\sim r^{-\eta}$ with the critical exponent $\eta=1/2$ [4–6]. Finite temperature phase transition has been predicted in the AFI model with higher spins [7,8]. Recently there has been a renewed interest on the present model with elastic distortions [9–12] or with a staggered field [13] in the context of glassy dynamics which may give insights into the nature of the glass transition. It should be emphasized that the macroscopic degeneracy of the ground state does not always guarantee a critical state. For example, the ground state of the AFI model on Kagomé lattice has extensive entropy, but is noncritical: spatial spin correlations decay exponentially. Although spatial connectivity is thought to have something to do with the existence of the critical phase (Kagomé lattice can be obtained from triangular lattice by removing sites in a regular manner), it remains an open question as to what conditions are required to have a critical state [14–16].

It has been shown [13] that via a dimer-covering method [17] the macroscopically degenerate ground states of the triangular AFI model can be classified into sectors characterized by string density p. In any ground state only two bonds satisfy the AF interaction in each plaquette. Since two neighboring plaquettes always share a common bond, as shown in Fig. 1(a), one can draw a line (dimer) from the center of one plaquette to that of the other, intersecting the shared frustrated bond. Then every plaquette center becomes the end point of a dimer. Now we make a dimer-covering in the so-called "standard" ground state which has alternating up-spin rows and down-spin rows, as shown in Fig. 1(b). When these two dimer-covered configurations are superimposed, a string configuration shown in Fig. 1(c) is obtained.

The number of strings is conserved under local dynamics such as spin-flip or spin-exchange kinetics. Nor can the strings intersect with one another. It has been shown [13] that each ground-state sector has a unique number of strings. Therefore a ground state belonging to a certain sector cannot evolve into other ground states belonging to different sectors. The time evolution of a ground state is always confined within the sector which the initial ground state belongs to. In

*Present address: SUPA, School of Physics, University of Edinburgh, Edinburgh EH9 3JZ, UK.

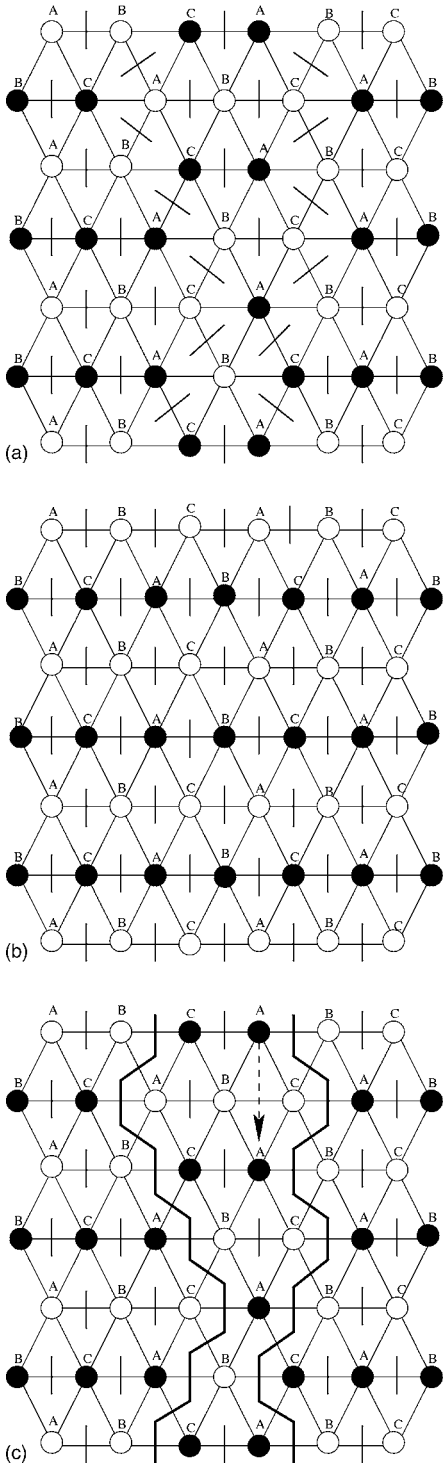

FIG. 1. (a) As an initial step for constructing a string representation (through dimer covering) for a given ground state configuration, one draws a line (dimer) from one center of a plaquette to the center of a neighboring plaquette when the shared bond (between the two neighboring plaquettes) does not satisfy the antiferromagnetic interaction (in other words, the two spins for the bond are parallel). (b) As the second step, one constructs a dimer covering [in the same way as in (a)] for the so-called "standard" ground state which has alternating up-spin rows and down-spin rows. (c) Finally, one combines the results of the above two steps to get the final string representation.

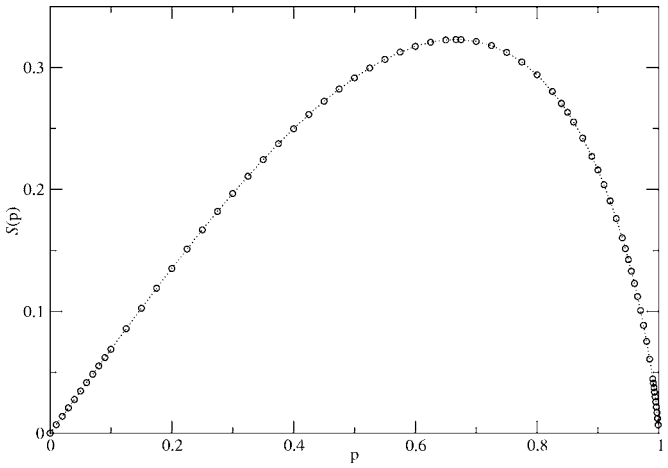

FIG. 2. The entropy density $\mathcal{S}(p)$ as a function of the string density p, obtained from a numerical integration of Eq. (2). $\mathcal{S}(p)$ becomes maximum at $p=2/3$, and the maximum entropy $\mathcal{S}(2/3)=0.323066$.

this sense, the dynamics within the ground state manifold is nonergodic. However, since each sector with nonzero string density has infinite number of ground states, one may regard each sector as an ergodic component: the dynamics is ergodic within each sector. One can thus talk about a "restricted" equilibrium in each sector. The number of ground states in a sector with string density p, $\mathcal{N}(p)$, has been exactly computed using a transfer matrix method as $\mathcal{N}(p)=\exp[N\mathcal{S}(p)]$, N being the number of spins with the entropy density given by an integral [13]

$$\mathcal{S}(p) = \int_0^p \ln\left[2\cos\left(\frac{\pi}{2}x\right)\right]dx. \tag{2}$$

Figure 2 shows the entropy density $\mathcal{S}(p)$ as a function of p, which is obtained from numerical integrations of Eq. (2). $\mathcal{S}(p)$ becomes maximum at $p=2/3$ with the maximum entropy $\mathcal{S}(2/3)=\int_0^{2/3}\ln[2\cos(\frac{\pi}{2}x)]dx=0.323066$ is the entropy derived by Wannier [2] five decades ago. The entropy density is linearly proportional to the string density as $\mathcal{S}(p)=(\ln 2)p$ for small p, whereas its derivative with respect to p tends to diverge as p approaches unity. The exponential dependence on N of the degeneracy implies that the sector with $p=2/3$ dominates other sectors in its number of states. We thus call the sector with $p=2/3$ the dominant or major sector, and call the other sectors the "minor" ones.

In a recent work [18] we focused on the kinetic aspects of the model, attempting to characterize the nonequilibrium critical dynamics of the model using a single spin-flip Monte Carlo kinetics. Here we recapitulate what we have observed in that work. We first examined the kinetics ensuing from an instantaneous quench starting from high-temperature disordered initial states to the zero temperature. Initial disordered state has high population of local defects [19] which are identified as unit plaquettes with the three spins at corners having the same up or down directions. Via pair annihilation of defects the system evolves towards the equilibrium ground states (belonging to the dominant sector). A unique

feature of the kinetics here is that due to the macroscopic degeneracy of the ground states the background configuration on which defects move, fluctuates via frequent flips of the so-called loose spins [20] whose flip requires no energy cost. We found that these fluctuations of the loose spins interact with defect motions and thereby significantly affect the diffusive properties of the defects. The kinetics reveals a single growing length scale $\xi(t)$, the nonequilibrium spin correlation length, which can be extracted from the dynamic spin correlation function $C(r,t)$. From the viewpoint of defects, this length scale can be regarded as the mean separation between defects. The kinetic process exhibits a self-similarity under rescaling of the distance with $\xi(t)$, which is manifested in the scaling collapse of $C(r,t)$ for various times t as $C(r,t)=r^{-\eta}F(r/\xi(t))$ with $\eta=1/2$. The scaling function $F(x)$ is independent of time t.

One controvertial aspect of the nonequilibrium kinetics is the time dependence of the growing length scale $\xi(t)$. Earlier simulation work by Moore *et al.* [21] contends that the kinetics is the same as that observed in the two-dimensional XY model, and therefore that the length grows in time as $\xi(t)=(t/\ln t)^{1/z}$ with the dynamic exponent $z=2$ [22–25] which exhibits a logarithmic correction. Contrary to this viewpoint, the present authors [18] have argued that $\xi(t)$ exhibits a genuine subdiffusive power law growth (without logarithmic correction), $\xi(t)\sim t^{1/z}$ with $z\simeq 2.33$. In particular, we attributed this subdiffusive growth to the mutual interaction of defects and loose spins. We argued that this interaction makes the defects perform a restricted random walk: the ground state fluctuations via loose spins induce microscopic blocking (on average) of the defect motion. Further works are needed to fully understand the nature of defect motion in the present model.

We have also considered the nonequilibrium relaxation dynamics within the ground state ensemble, focusing on the relaxation within the dominant sector with $p=2/3$. The initial state employed was a ground state in which the strings are straight and regularly spaced so that the intial state has maximum number density of the loose spins $\rho_l(t=0)=p=2/3$, as shown in Fig. 3(a). For this initial configuration, all spins in each sublattice A, B, C have the same sign, and hence each sublattice is fully ordered. Thus the two sublattice magnetizations (A and B) are equal and opposite to the third sublattice magnetization: $m_A=m_B=-m_C=1$, which is subject to permutation symmetry of the three sublattices. Since the initial configuration is a ground state, it has *no* defects, and the time evolution proceeds via flips of the loose spins only. In order to probe the nonequilibrium relaxation from this "ordered" initial state, we measured the nonequilibrium spin correlations in each sublattice. In fact, by permutation symmetry these correlation functions are the same. Hence let us call any one of them as $C(r,t)$. At a given time t, the correlation function $C(r,t)$ approaches a nonzero value at large distances which is actually the square of sublattice magnetization $m_S^2(t)$. This saturation sets in at larger distances for late times. This means that the nonequilibrium correlation length $\xi(t)$ of spin fluctuations grows in time. We found that the correlation of spin fluctuations $C_F(r,t)\equiv C(r,t)-m_S^2(t)$ also shows a critical dynamic scaling behavior $C_F(r,t)=r^{-\eta}G(r/\xi(t))$, where $\xi(t)$ grows diffusively in time, i.e., $\xi(t)\sim t^{1/z}$ with $z=2$. This purely diffusive growth of the correlation length should be contrasted with the subdiffusive growth of the correlation length in the presence of annihilating defects. The critical dynamic scaling implies that the sublattice magnetization should decay algebraically in time as $m_S^2(t)\sim t^{-\eta/z}$ with $\eta/z=1/4$. We therefore observed an interesting initial state dependence of the kinetics, which is due to highly complex structure of the degenerate ground states.

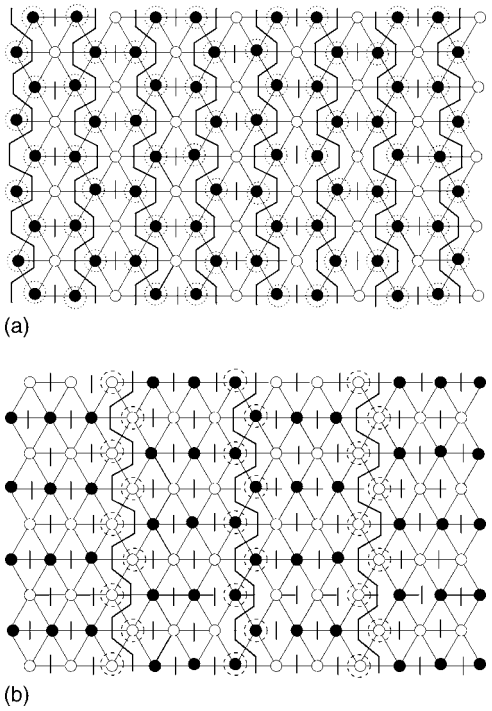

FIG. 3. (a) One of the ground state configurations with the string number density $p=2/3$ that is employed as the initial state for the nonequilibrium relaxation dynamics within the dominant sector of the ground state ensemble. This configuration can be considered as the maximally ordered state in the sense that the lattice can be decomposed into three (A, B, and C) regular triangular sublattices each of which is fully ordered (e.g., two with up spins and the other with down spins). Encircled are the loose spins whose flips do not cost energy. (b) One example of the ground state configurations with the string number density $p=1/3$ that is employed as the initial state for the nonequilibrium relaxation dynamics within the corresponding sector of the ground state ensemble.

In the present work we extend our aforementioned previous study to minor sectors with $p=1/(3n)$ with $n=1,2,\ldots$. We aim to characterize the nonequilibrium kinetics of the system evolving towards the equilibrium state within each minor sector under single spin-flip kinetics. In particular we focus on distinct dynamic features compared to those observed in the dominant sector with $p=2/3$. We find that, as p is reduced from 2/3, the relaxation dynamics as well as the final equilibrium spatial correlation functions exhibit a characteristic spatial anisotropy between the direction parallel to the initial strings (vertical direction in our definition) and the horizontal direction which is perpendicular to the strings. Accordingly, the dynamic spatial correlation

functions measured along the vertical and horizontal directions can be separately collapsed into distinct scaling functions. As a by-product we obtain an analytic form for the equilibrium spatial correlation function. This can be regarded as a generalization of the equilibrium spatial correlation functions for $p=2/3$ [4]. In the equilibrium correlation functions, the correlation length scale $\xi_{e,V}(p)$ along the vertical direction tends to diverge with vanishing string density as $\xi_{e,V}(p)\sim p^{-2}$, while in contrast, the length scale $\xi_{e,H}(p)$ along horizontal direction exhibits a divergence with $\xi_{e,H}(p)\sim p^{-1}$ which is proportional to the separation between neighboring strings.

Along the vertical direction, in the minor sectors, the equilibrium spin correlation function exhibits a slower relaxation in the short distance. As argued below, this turns out to be another type of critical relaxation. The same critical relaxation as that in the dominant sector is recovered at larger distance. This new critical region becomes larger as p is reduced, diverging as inverse square of p as mentioned above. The same type of behavior is reflected in the temporal relaxation of the spin autocorrelation function. When p is smaller than but close to $p=2/3$, the corresponding critical behavior starts to appear in the short time regime, and after that the relaxation shows the same critical behavior as in the case of $p=2/3$. As p becomes further reduced, this new critical regime (in time) gets larger, but the late-stage critical relaxation is recovered in the long-time limit, as in the case of spatial relaxation. When p is small enough, however, we are not able to observe the eventual crossover to the long-time critical relaxation within our simulation window. We also find that the spin autocorrelation functions show a simple scaling behavior when the time is rescaled with respect to the growing time scale (with reduced string density). That is, we have $A(t)=\mathcal{A}(t/\tau_A(p))$ with the time scale $\tau_A(p)$ growing with vanishing p as $\tau_A(p)\sim p^{-\phi}$ with ϕ very close to 4. As argued in detail below, the power law dependence of $\xi_{e,V}(p)$, $\xi_{e,H}(p)$, and $\tau_A(p)$ on the string density p can be understood in terms of random walk nature of the string motions within the limiting range of the average distance between neighboring strings.

II. THE INITIAL GROUND STATES

We perform dynamic Monte Carlo simulations on the AFI model on a triangular lattice using a single spin-flip Metropolis kinetics at zero temperature: the spin flip without energy cost is accepted, whereas the flip resulting in positive energy cost is rejected. In most simulations, we use lattices with linear dimension $L=1296$ (unless otherwise specified), and employ the periodic boundary conditions in both horizontal and vertical directions.

Figures 3(a) and 3(b) show examples of the initial ground states used in our simulations. The string density p is defined as $p=N_S/L$ where N_S is the total number of strings. The initial states are such that all strings are straight and evenly distributed. Each string forms a chain due to the periodic boundary condition in the vertical direction. Here we make a comment on one subtle point on the string density. In the case where one employs periodic boundary conditions along both horizontal and vertical directions (i.e., in torus geometry), the strings can have finite density along *both* directions resulting in strings that are not parallel (in the average sense) to the vertical direction but have finite average slope with winding number larger than unity. Therefore for a given string density, the ground state will further be classified into sectors with different winding numbers. In this work, however, for simplicity, we focus only on the case of unit winding number where the strings are parallel on the average to the vertical direction.

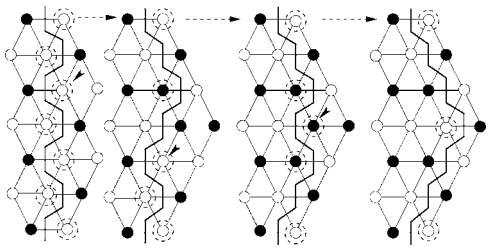

FIG. 4. This shows how flips of loose spins make a string move and thereby penetrate into the initially immovable regions between the strings. In the first (left-most) figure, one observes that if a loose spin is flipped, while it is still a loose spin, its NN loose spins are no longer loose spins. This can be regarded as annihilation of the loose spins. The second and the third figures indicate that the flip of a loose spin can create a loose spin in one of its NN sites. Finally, in the fourth (rightmost) figure, a straight string can bend over and penetrate into the previously frozen spin region. Encircled are the loose spins.

The relaxation proceeds via flips of the loose spins only. A loose spin is defined as the spin whose flip costs zero energy, and it can be identified as the spin whose six NN spins alternate in their signs, which are encircled in Fig. 3(a) or 3(b). Note that loose spins are *always* located at the "kink" segments of each string. Therefore the initial loose spin density is the same as the string density, i.e., $\rho_l(0)=p$, which is the maximum loose spin density in that sector. Between the strings are the domains of the stripe phase which has alternating lines of up and down spins. Apart from the loose spins located at the kinks of strings, there exist no loose spins in the stripe domains since any spin flip in the domains creates a pair (or pairs) of defects.

Figure 4 shows some elementary processes of how flips of loose spins make a string move and thereby penetrate into the initially immovable regions between the strings. In the first figure of Fig. 4, one observes that if a loose spin is flipped, while it is still a loose spin, its NN loose spins are no longer loose spins. This can be regarded as annihilation of loose spins. The second and the third figures indicate that the flip of a loose spin can create a new loose spin in one of its NN sites. The number of the loose spins is therefore not conserved. Through several steps of processes, a straight string can bend over and penetrate into the previously frozen spin region. Shown in Fig. 5 are snapshots of loose-spin configurations for $p=1/18$.

III. RESULTS AND DISCUSSIONS

A. Spatial relaxation of spin ordering in the major sector

Equilibrium spatial correlation function (along the three major axes) has been given by Stephenson [4] as

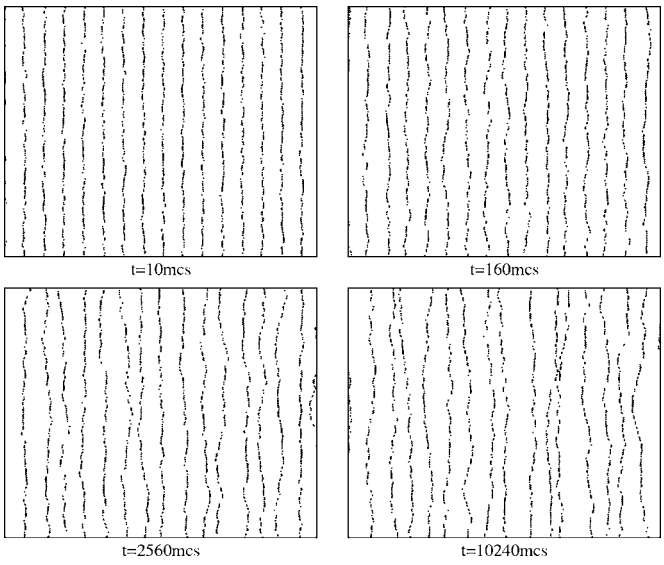

FIG. 5. Snapshots of loose-spin configurations for $p=1/18$.

$$C_e(r) \sim r^{-\eta} \cos\left(\frac{2\pi r}{3}\right) \tag{3}$$

which represents an isotropic critical decay and additional modulation term with spatial period 3. Here, we investigate the nonequilibrium relaxation dynamics of the system with the initial state of $p=2/3$ such that all spins in each of the three sublattices A, B, and C, respectively, have the same sign, and hence each sublattice is fully ordered, i.e., $m_A=m_B=-m_C=1$. For convenience of simulations and scaling fit, we can probe the relaxation of the spin ordering by measuring the correlation of spins belonging to the same sublattice along three major axes (ignoring the modulation term): we measured the spin correlation functions at time t

$$C_A(r,t) = \left\langle \sum_{i\in A} \sigma_i(t)\sigma_{i+r}(t) \right\rangle \Big/ (N/3), \quad r=3n, \tag{4}$$

where $n=0,1,2,3,\ldots$. This correlation function is obtained from the average over measurements along three major directions of the triangular lattice. One can measure $C_B(r,t)$ and $C_C(r,t)$ in the same manner. It is expected that these three correlation functions be the same due to the permutation symmetry of the three sublattices. In accordance with this expectation, we find their numerical results almost indistinguishable, and the presented result is the average of these three functions, denoted by $C(r,t)$. By definition, then, we have $C(0,t)=C(r,t=0)=1$. Since two spins separated by large distance are uncorrelated, $C(r,t)$ will depend only on time t for large distances $C(r,t)\equiv m_S^2(t)$ for $r \gg \xi(t)$, where $m_S(t)$ is the sublattice magnetization and $\xi(t)$ is the correlation length at time t.

We find that $C(r,t)$ obeys a critical dynamic scaling of the form

$$C(r,t) - m_S^2(t) = r^{-\eta} F(r/\xi(t)), \quad \eta = 1/2, \tag{5}$$

where $F(x)$ is the scaling function. The algebraic factor $r^{-\eta}$ reflects the critical equilibrium spin correlation. The correlation length $\xi(t)$ is found to exhibit a diffusive growth in time as

$$\xi(t) \sim t^{1/z}, \quad z=2. \tag{6}$$

Using the critical scaling (5), one can readily show that the sublattice magnetization $m_S(t)$ exhibits a power-law relaxation

$$m_S^2(t) \sim t^{-\eta/z} \sim t^{-1/4}. \tag{7}$$

B. Spatial relaxation of spin ordering in the minor sectors

Contrary to the initial state with $p=2/3$, as one can see from Fig. 3(b), in the initial states belonging to the minor sectors, spins in each sublattice no longer have the same sign. Instead, we have an obvious anisotropy in the spatial spin arrangement in the initial state. Interestingly we find that the anisotropy in the spatial correlation persists even in the long time limit of equilibrium. Here, we look at the nonequilibrium relaxation of this spatial spin correlation along the following three directions of main interest: along the vertical direction parallel to the strings in the initial state, along the horizontal direction perpendicular to the vertical direction (along one of the three triangular axes), along one of the remaining diagonal triangular axes (which lies 60° north of east).

1. Vertical direction

To begin with, let us deal with the spatial spin correlation along the vertical direction defined as

$$C_V(r,t) = \frac{1}{N}\left\langle \sum_{i=1}^{N} \sigma_i(t)\sigma_{i+\vec{r}}(t) \right\rangle, \quad \vec{r} = \hat{y}\sqrt{3}n, \tag{8}$$

where the separation $\vec{r}$ lies along the vertical direction ($\hat{y}$ being the unit vector in the vertical direction) with magnitude $r\equiv|\vec{r}|=\sqrt{3}n$ with $n=0,1,2,\ldots$. Figure 6 shows $C_V(r,t)$ for $p=2/3,1/3,1/6,1/9,1/18$ in log-log scale. Note that there exists some range of distance r in which $C_V(r,t)$ shows the same r dependence for different times, i.e., the correlation function exhibits no time dependence. This means that the system is equilibrated within this distance. Naturally this equilibrated region becomes larger at longer times. Therefore $C_V(r,t)$ maps out the equilibrium spin correlation function $C_{e,V}(r)$ for each p. For example, Fig. 6 demonstrates that $C_{e,V}(r)$ for $p=2/3$ exhibits a critical relaxation $C_{e,V}(r)\sim r^{-\eta}$ with $\eta=1/2$, in accordance with the theoretical prediction. Compared to this critical relaxation for the case of $p=2/3$, the spatial relaxation of $C_{e,V}(r)$ in the minor sectors becomes much slower with smaller p. It is expected that for minor sectors the system relaxes with slower rate due to fewer strings and hence fewer loose spins. It is interesting to observe in Fig. 6 that another type of spatial relaxation in $C_{e,V}(r)$ starts to emerge in the short distance region, which becomes larger as p becomes smaller. At long distances, for some values of p such as $p=1/3,1/6,1/9$, $C_{e,V}(r)$ is observed to cross over to the same critical relaxation

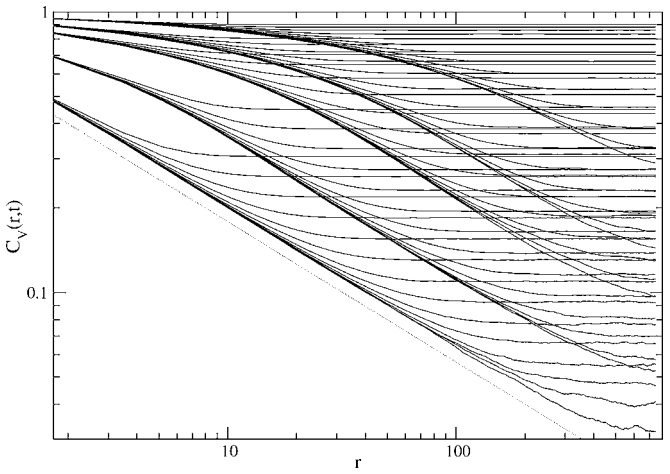

FIG. 6. $C_V(r,t)$ for $p=2/3,1/3,1/6,1/9,1/18$ (from below) in log-log scale. In the minor sectors, critical relaxation of the equilibrium correlation function $C_{e,V}(r)$ starts to emerge in the short distance region, and grows as the string density p becomes smaller. At long distances, for values of p such as $p=1/3,1/6,1/9$, $C_{e,V}(r)$ is observed to cross over to the same critical relaxation $C_{e,V}(r) \sim r^{-\eta}$ with $\eta=1/2$ (dotted line) as in the case of $p=2/3$.

$C_{e,V}(r) \sim r^{-\eta}$ with $\eta=1/2$ as that observed in the major sector. In fact, as discussed below (Sec. II C 2), this short-distance relaxation is a new critical relaxation which arises from unrestricted random walk motion of the strings. However, for further reduced density $p=1/18$ the recovery of the late-stage critical relaxation is not yet observed since for this small value of p the spatial extent of the early-stage critical relaxation becomes very large. However, it is certain for this case that the late-stage critical relaxation will be eventually observed with bigger system size and longer simulation time.

As demonstrated in Fig. 7, we find that $C_{e,V}(r)$ obeys a simple scaling of the form $C_{e,V}(r)=f_{e,V}(r/\xi_{e,V}(p))$, where the length scale $\xi_{e,V}(p)$ is defined as $C_{e,V}(r=\xi_{e,V})=C_0$ where C_0 is set to be $C_0=0.5$ for convenience. Note from Fig. 6 that by

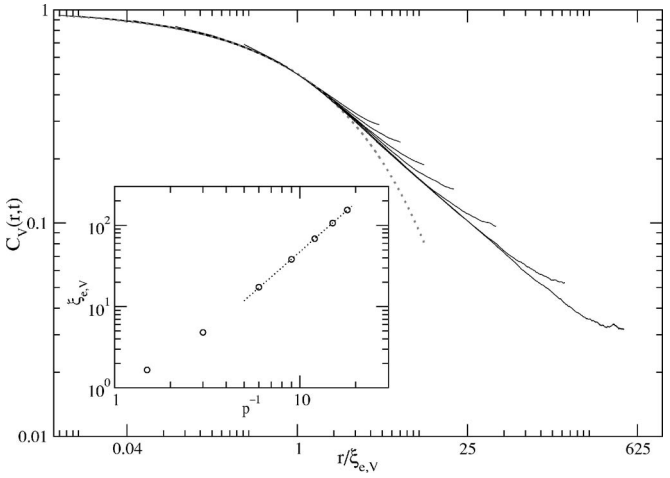

FIG. 7. A simple scaling fit of the form $C_{e,V}(r)=f_{e,V}(r/\xi_{e,V}(p))$ with $\xi_{e,V}(p)$ defined as $C_{e,V}(r=\xi_{e,V})=C_0$ (C_0 is set to be $C_0=0.5$). The inset shows the $\xi_{e,V}(p)$ vs p^{-1} where $\xi_{e,V}(p)$ is found to grow with smaller p diverging as $\xi_{e,V}(p) \sim p^{-\phi}$ with $\phi \simeq 2.0$.

the above definition of $\xi_{e,V}(p)$, $\xi_{e,V}(p)$ is inside the first critical region for each $p<2/3$. This equilibrium correlation length $\xi_{e,V}(p)$ is found to grow with smaller p and tend to diverge as $\xi_{e,V}(p) \sim p^{-\phi}$ with $\phi \simeq 2.0$, as shown in the inset of Fig. 7. The scaling of the critical part of $C_{e,V}(r)$ for various values of p including $p=2/3$ implies that the amplitude of the critical relaxation is inversely proportional to the string density p since $C_{e,V}(r) \sim p^{-1} r^{-1/2} \sim (rp^2)^{-1/2}$. As for the power law divergence of $\xi_{e,V}(p) \sim p^{-2}$ in the limit of small p, we can argue as follows. The average distance h_0 between neighboring strings scales as $h_0 \sim 1/p$. Now the horizontal fluctuations of the strings can be regarded as a random walk in the equilibrium situation, and therefore the typical length scale along the direction of the strings that corresponds to a horizontal fluctuation h_0 can be considered as the spin correlation length $\xi_{e,V}(p)$. Therefore from the random walk nature we can write as $h_0 \sim \xi_{e,V}^{1/2}(p)$ which gives $\xi_{e,V}(p) \sim h_0^2 \sim 1/p^2$ consistent with the above simulation results.

The shape of the scaling function $f_{e,V}(x)$ is such that, while $f_{e,V}(x)$ is given by a power law decay $f_{e,V}(x) \sim x^{-1/2}$ for $x \gg 1$, it is found to be well fitted by the form $f_{e,V}(x)=1-x^{\gamma} \simeq \exp(-x^{\gamma})$ with $\gamma \simeq 0.5$ for $x \ll 1$. The above scaling of $C_{e,V}(r)$ with respect to the length $\xi_{e,V}(p)$ tells us that the early-stage critical spatial region diverges with vanishing p as p^{-2}. As we see below, this emergence and growth of the early-stage critical relaxation and the final crossover to the late-stage critical relaxation in both spatial and temporal regimes is one of the main features of the relaxation in the minor sectors. Short distance behavior of the scaling function $f_{e,V}(x) \simeq 1-x^{\gamma}$ with $\gamma \simeq 0.5$ can also be understood in a similar manner as follows. As before we assume that each string performs a random walk in the horizontal direction with the restriction of maximal displacement of order h_0. Now, we take a short bar of length r parallel to the vertical direction and consider the probability $P(r)$ that the bar crosses a string. Since the horizontal displacement Δh of the string for the vertical length scale r corresponding to the length of the bar, scales as $\Delta h \sim r^{1/2}$, we have $P(r) \propto \Delta h/h_0 \sim pr^{1/2}$. Therefore $C_{e,V}(r)$ at short distance r can be written as $C_{e,V}(r) \simeq 1(1-P(r))+(-1)P(r)=1-2P(r) \simeq 1-cpr^{1/2}=1-c(r/\xi_{e,V}(p))^{1/2}$ with c being a constant. This explains the short-distance behavior of $f_{e,V}(x) \simeq 1-x^{\gamma}$ with $\gamma \simeq 0.5$.

The nonequilibrium spatial correlations along the vertical direction are expected to follow the scaling behavior

$$C_V(r,t) = C_{e,V}(r) g_V(r/\xi_V(t,p)), \tag{9}$$

where $\xi_V(t,p) \sim p^2 t^{1/2}$ is the diffusively growing length scale. The scaling function $g_V(x)$ behaves as $g_V(x) \sim x^{1/2}$ as $x \to \infty$ and $g_V(x) \simeq 1$ as $x \to 0$.

2. Horizontal direction

Next we go to the spatial spin correlation function $C_H(r,t)$ along the horizontal major axis

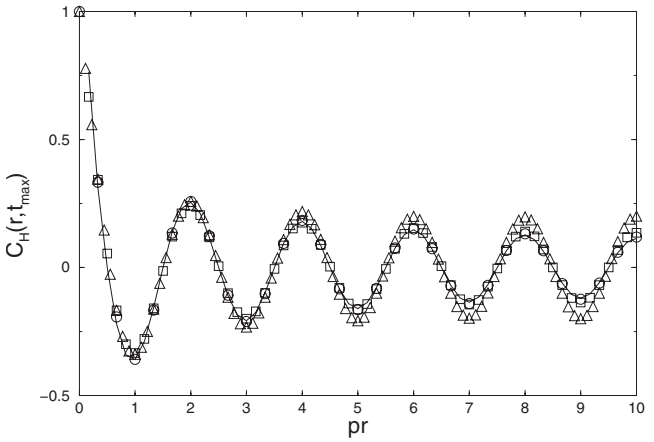

FIG. 8. $C_H(r,t_{\max})$ vs pr for three different values of p [$p=1/3$ (circle), $1/6$ (square), $1/9$ (triangle)] at $t_{\max}=81,920$ (mcs). Solid line represents $C_{e,H}(r)=A_H(pr)^{-1/2}\cos(\pi pr)$ with $A_H=0.35$. For $p=1/9$ the equilibrated region is shorter compared to the cases of the other two values of p.

$$C_H(r,t)=\frac{1}{N}\left\langle \sum_{i=1}^{N}\sigma_i(t)\sigma_{i+\vec{r}}(t)\right\rangle, \quad \vec{r}=n\hat{x}, \tag{10}$$

where the separation $\vec{r}$ lies along the horizontal axis ($\hat{x}$ being the unit vector in the horizontal direction). Here, in contrast to the case of vertical direction, we observe a clear modulation in the correlation function with spatial period proportional to p^{-1} which is of the order of the spacing between neighboring strings. As shown in Fig. 8, from the behavior of the spatial correlation in the long time limit, we find that the spatial correlation function $C_{e,H}(r)$ at equilibrium can be fitted by

$$C_{e,H}(r)\sim p^{-1/2}r^{-1/2}\cos(p\pi r), \tag{11}$$

where the modulation factor of $\cos(p\pi r)$ clearly reflects the existence of strings with average separation $d_S\sim 1/p$. The expression (11) is a generalization of Eq. (3) which holds for $p=2/3$ to the case of minor sectors with $p<2/3$. We mention that in a recent independent work [26] Eq. (11) was analytically obtained by viewing the present model as the one-dimensional coupled chains of topological objects. Equation (11) can be rewritten in a scaling form as

$$C_{e,H}(r)=f_{e,H}(r/\xi_{e,H}(p)) \tag{12}$$

with the scaling function $f_{e,H}(x)\sim x^{-1/2}\cos(\pi x)$ and the correlation length scale $\xi_{e,H}(p)\sim 1/p$.

Now, the nonequilibrium spatial correlations along the horizontal direction are expected to obey the scaling behavior

$$C_H(r,t)=C_{e,H}(r)g_H(r/\xi_H(t,p)), \tag{13}$$

where $\xi_H(t,p)\sim pt^{1/2}$ is the diffusively growing length scale as in the case of the spatial correlation along the vertical direction. The scaling function $g_H(x)$ behaves as $g_H(x)\sim x^{1/2}$ as $x\to\infty$ and $g_H(x)\simeq 1$ as $x\to 0$.

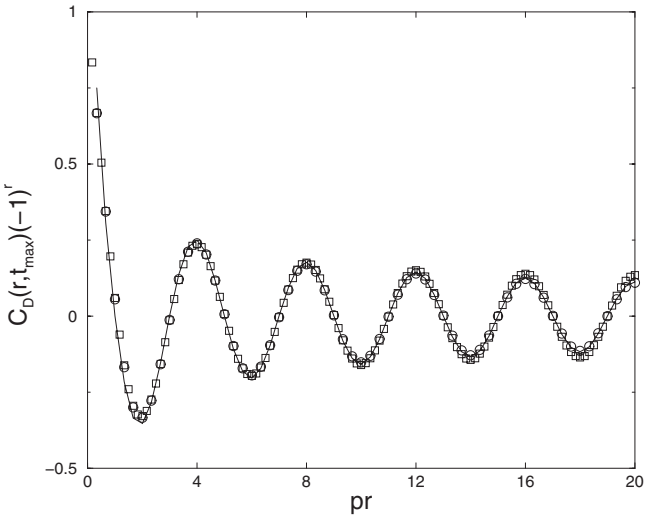

FIG. 9. $C_D(r,t_{\max})$ vs pr for $p=1/3$ (circle) and $p=1/6$ (square) at $t_{\max}=81,920$ (mcs). Solid line represents $(-1)^r C_{e,D}(r)=A_D(pr)^{-1/2}\cos(\pi pr/2)$ with $A_D=0.5$.

3. Diagonal direction

Finally, we consider the spatial spin correlation $C_D(r,t)$ along the diagonal triangular axis at 60°

$$C_D(r,t)=\frac{1}{N}\left\langle \sum_{i=1}^{N}\sigma_i(t)\sigma_{i+\vec{r}}(t)\right\rangle, \quad \vec{r}=\left(\frac{1}{2},\frac{\sqrt{3}}{2}\right)n. \tag{14}$$

Along this axis, we get the following form of equilibrium correlation function (see Fig. 9):

$$C_{e,D}(r)\sim p^{-1/2}r^{-1/2}\cos\left(\frac{p}{2}\pi r\right)(-1)^r \tag{15}$$

which fits very well the long time limit of $C_D(r,t)$. Here, r measures the distance along the diagonal axis with the unit lattice constant set equal to 1. Nonequilibrium relaxation of the spatial correlation $C_D(r,t)$ satisfies a critical dynamic scaling that is similar to the case of the correlations along the horizontal axes. The equilibrium spatial correlation functions along the three different directions can be combined into the following form:

$$C_e(\vec{r})\sim r^{-1/2}\cos(p\pi x)(-1)^y, \tag{16}$$

where $\vec{r}\equiv(x,y)$ and $r\equiv|\vec{r}|$.

C. The spin auto-correlation function

1. The major sector

We have measured the relaxation of the spin autocorrelation function $A(t)$ which measures temporal correlation between the initial spin configuration and the spin configuration at time t:

$$A(t)=\frac{1}{N}\left\langle \sum_{i=1}^{N}\sigma_i(0)\sigma_i(t)\right\rangle. \tag{17}$$

For the case of the dominant sector, each sublattice is fully ordered for the initial state. Therefore it is easy to show that

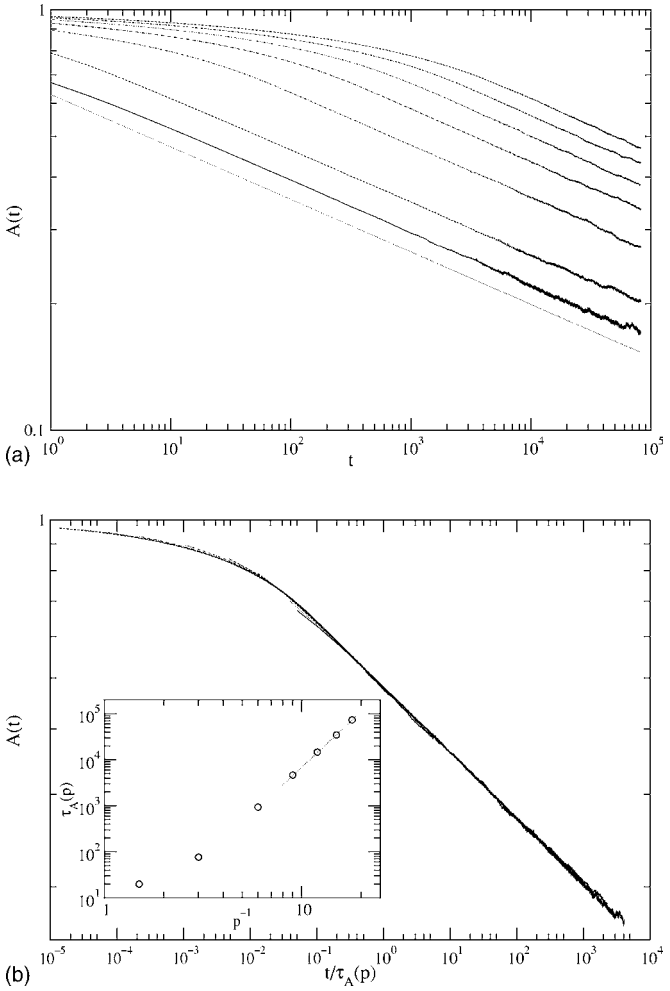

FIG. 10. (a) The relaxation of the spin autocorrelation function $A(t)$ for various values of p having the same values as in Fig. 6. As p is further reduced from $p=2/3$, the early-stage critical relaxation starts to appear in the short time regime. However, for all p, we observe that the relaxation tends to $A(t)\sim t^{-\eta/2z}\sim t^{-1/8}$ (dotted line) in the late time regime. (b) A scaling attempt of $A(t)$ for various values of p with respect to the characteristic time scale $\tau_A(p)$ defined as $A(t=\tau_A(p))=0.5$, where we find an excellent scaling collapse with a time string-density superposition $A(t)=\mathcal{A}(t/\tau_A(p))$. The inset shows $\tau_A(p)$ vs p^{-1} exhibiting a power law divergence of $\tau_A(p)\sim p^{-\phi}$ with $\phi\simeq 3.96$ for small values of $p\leqslant 1/9$.

$$A(t)=\frac{1}{3}[m_A(t)+m_B(t)-m_C(t)], \tag{18}$$

where $m_A(t)$, $m_B(t)$, and $m_C(t)$ are the sublattice magnetizations, and we assumed that the initial spin configuration for $p=2/3$ is such that all spins are up (+1) for the sublattices A and B, and all spins are down (−1) for the sublattice C.

We have shown before that the critical dynamic scaling leads to the power law relaxation of the sublattice magnetization $m_A^2(t)=m_B^2(t)=m_C^2(t)\sim t^{-\eta/z}$ at long times with $\eta/z=1/4$, and hence $A(t)\sim t^{-\eta/2z}\sim t^{-1/8}$, in accordance with the result shown in Fig. 10(a).

2. The minor sectors

In the case of minor sectors, as in the spatial spin correlation functions, we see in Fig. 10(a) that as p is reduced from $p=2/3$ the early-stage critical relaxation starts to appear in the short time region, and expands its time region as p is further reduced. The behavior of $A(t)$ eventually crosses over to the same critical decay $A(t)\sim t^{-1/8}$ as observed in the dominant sector. This late-stage critical relaxation, for example, is seen for the last one decade of time for the case of the string density $p=1/18$. Shown in Fig. 10(b) is a scaling attempt of $A(t)$ for various values of string density p with respect to the characteristic time scale $\tau_A(p)$ defined as $A[t=\tau_A(p)]=0.5$. The scaling collapse is excellent: the spin autocorrelation function obeys a time string-density superposition $A(t)=\mathcal{A}(t/\tau_A(p))$. It is demonstrated in the inset of Fig. 10(b) that $\tau_A(p)$ shows a power law divergence as $\tau_A(p)\sim p^{-\phi}$ with $\phi\simeq 3.96$ for small values of string density $p\leqslant 1/6$.

The shape of scaling function $\mathcal{A}(x)$ with $\tau\equiv t/\tau_A(p)$ exhibits a stretched exponential relaxation $A(\tau)=\exp(-\tau^{0.25})$ for $\tau\ll 1$ and a critical relaxation $\mathcal{A}(\tau)\sim\tau^{-1/8}$ for $\tau\gg 1$. One can interpret $\tau_A(p)$ as the time scale at which the critical relaxation sets in. The power law dependence of $\tau_A(p)$ on the string density p, i.e., $\tau_A(p)\sim p^{-\phi}$ with $\phi\simeq 3.96$ can be understood as follows. Typical relaxation time for the spin autocorrelation function corresponds to the time scale during which a certain point on the string crosses the average distance h_0 between neighboring strings. Since, due to the random walk nature of the string configuration at short distance, the horizontal displacement $h(y,t)$ of a certain point on the string as a function of the vertical distance y can be thought of as satisfying an Edward-Wilkinson-type equation

$$\frac{\partial h}{\partial t}=D\frac{\partial^2 h}{\partial y^2}+\eta(y,t), \tag{19}$$

where D is the diffusion coefficient and $\eta(y,t)$ representing an uncorrelated Gaussian noise with zero mean. Therefore, typical relaxation time $\tau_A(p)$ for the spin autocorrelation would correspond to the time scale of relaxation of the oscillation of the string at the typical scale of an inverse wave vector which is just the spatial correlation length $\xi_{e,V}(p)$. Hence, $\tau_A(p)$ would scale in proportion to the square of the correlation length $\tau_A(p)\sim\xi_{e,V}^2(p)$, which, together with $\xi_{e,V}(p)\sim 1/p^2$, gives $\tau_A(p)\sim 1/p^4$ in reasonable agreement with our simulation result of $\phi\simeq 3.96$.

Now as for the short time ($\tau<1$) behavior of the scaling function of the autocorrelation function $\mathcal{A}(\tau)\simeq\exp(-\tau^{1/4})\simeq 1-\tau^{1/4}$, we can simply reverse the above argument for the relaxation time versus the inverse string density $1/p$ or the transverse [height $h(y)$] fluctuation scale. That is, we can safely assume that the autocorrelation function at short time scale [shorter than the relaxation time scale $t\ll\tau_A(p)$] goes as $A(t)=1[1-\mathcal{P}(t)]+(-1)\mathcal{P}(t)\simeq 1-2\mathcal{P}(t)$, where $\mathcal{P}(t)$ denotes the (average) probability that a string crosses a typical point in the system. Since the dominant fluctuations of the strings are along the horizontal direction, it is simple to see that $\mathcal{P}(t)$ is proportional to the average transverse displacement up to

time t. However, this is simply proportional to $t^{1/4}$ from the argument given above, which gives a behavior in agreement with our simulation results.

Now, when the typical horizontal fluctuation of the strings reaches the scale of separation between nearest neighbor strings, we can no longer apply the above picture of noninteracting fluctuating strings and we should take into account the repulsion between neighboring strings. It is known that the transverse fluctuations exhibit a logarithmic divergence corresponding to the logarithmic roughening in two dimensions [27]. We believe that this logarithmic divergence will correspond to the power law relaxation of the spin autocorrelation function in the late time regime.

D. The loose spin density

For $p \leqslant 2/3$ the initial loose spin density is the same as the string density p. Figure 11(a) shows the relaxation of the loose spin density $\rho_l(t)$ for various values of p. $\rho_l(t)$ exhibits a slow monotonic decay toward a nonvanishing asymptotic value $\rho_l(t=\infty)(p)$ for each p. Previously, we have shown that, for the case of the dominant sector, $\rho_l(t)$ shows a power law relaxation approaching its equilibrium value as $\rho_l(t) = \rho_l(\infty) + \text{const}\, t^{-\alpha}$ with $\alpha \simeq 1.0$. The asymptotic value $\rho_l(\infty)$ was found to be $\rho_l(\infty) \simeq 0.29$. As for the initial states belonging to the minor sectors, one may get a hint from Fig. 4 that the dominant process for short times will be independent flips of well separated loose spins. Then each flip will remove two loose spins. If only this process were to continue, then the asymptotic value $\rho_l(\infty)$ would be $p/2$. As shown in Fig. 11(b), the time region in which $\rho_l(t)$ exhibits a power law decay $\rho_l(t) = p/2 + \text{const}\, t^{-1/2}$ is observed, becomes expanded as p is further reduced since the initial loose spin density is reduced accordingly. However, this relaxation crosses over to the same relaxation $\rho_l(\infty) + \text{const}\, t^{-1}$ as observed in the case of $p=2/3$. The asymptotic value $\rho_l(\infty)$ becomes very close to $p/2$ as p becomes very small. The noncritical time region becomes longer as p is getting smaller. But in this case it is rather difficult to measure the noncritical time region with varying p.

E. The persistence property

How long does a spin maintain its initial state without any flip during the time evolution? This question touches upon an interesting nonequilibrium dynamic aspect known as the persistence. This persistence property can be quantified by measuring $\rho_p(t)$, the number density of spins which are never flipped up to time t. It is found that for a variety of spin systems $\rho_p(t)$ exhibits power law relaxation in time $\rho_p(t) \sim t^{-\theta}$. The new nonequilibrium exponent θ has been analytically or numerically computed. For example, in the zero-temperature coarsening of the ferromagnetic Ising model $\theta = 3/8 = 0.375$ in one dimension [28], and $\theta \simeq 0.22$ for the two-dimensional square lattice [29].

In order to compute the density of persistent spins, we first define a local quantity $n_i(t) \equiv [1 + \sigma_i(0)\sigma_i(t)]/2$ [30] for each lattice site i. Obviously, $n_i(0) = 1$ for all sites. If the Ising spin $\sigma_i(t)$ is flipped at time t, then $n_i(t)$ becomes zero.

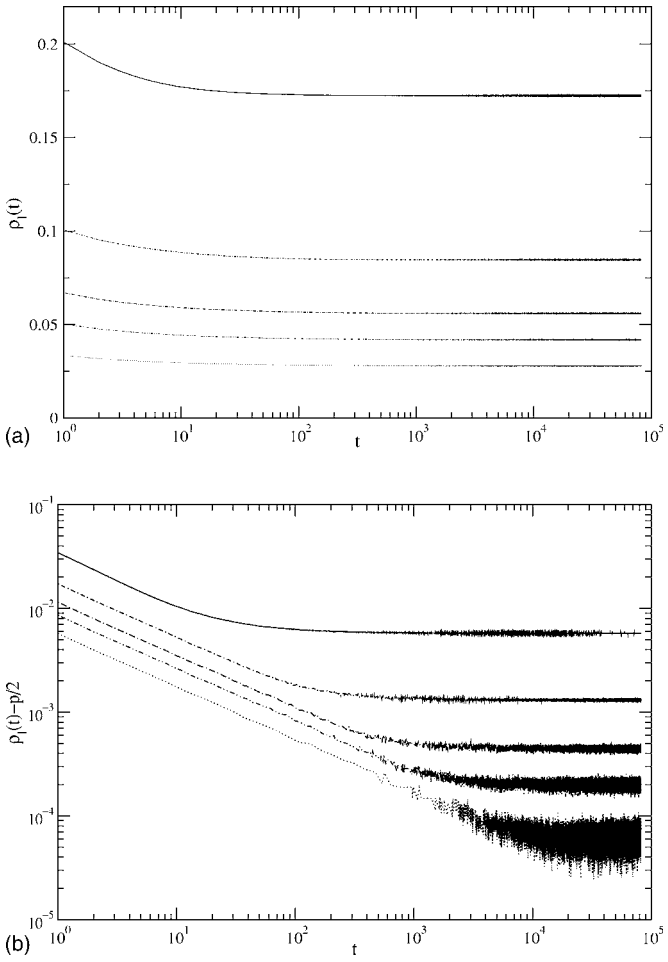

FIG. 11. (a) The relaxation of the loose spin density $\rho_l(t)$ for various values of the string density p. $\rho_l(t)$ exhibits a slow monotonic decay toward a nonvanishing asymptotic value $\rho_l(t=\infty)(p)$ for each p. (b) $\rho_l(t) - p/2$ vs t for $p = 2/3, 1/3, 1/6, 1/9, 1/18$ (from above). We observe a power law decay $\rho_l(t) = p/2 + \text{const}\, t^{-1/2}$, where the power law region becomes expanded as p is further reduced (because the initial loose spin density is reduced accordingly). But this relaxation crosses over to the same relaxation $\rho_l(\infty) + \text{const}\, t^{-1}$ as observed in the case of $p=2/3$.

Once it happens, we let $n_i(t)$ maintain the value zero even after regardless of subsequent flips of $\sigma_i(t)$. If $\sigma_i(t)$ is never flipped up to time t, then $n_i(t) = 1$. Therefore the number of persistent spins at time t is the sum of the sites with $n_i(t) = 1$. Hence $\rho_p(t) = \langle \Sigma_{i=1}^{N} n_i(t) \rangle / N$.

Shown in Fig. 12(a) is $\rho_p(t)$ for various values of p. For the case of the dominant sector, after an early transient relaxation $\rho_p(t)$ exhibits an exponential relaxation, which is well fitted by $\rho_p(t) = A_0 \exp(-t/\tau_0)$ with $A_0 \simeq 0.52$ and $\tau_0 \simeq 14.65$. This exponential decay can be attributed to fast flips of loose spins highly populated in the initial configuration. As p is reduced from $p=2/3$, the initial population of loose spins is reduced, and at the same time, the zero-loose spin domains between strings are enlarged. We find that the slow relaxation of $\rho_p(t)$ for the case of minor sectors can be well fitted by a stretched exponential function of the form $\rho_p(t) = A \exp(-(t/\tau)^{\beta})$ with $\beta < 1$. The amplitude A remains

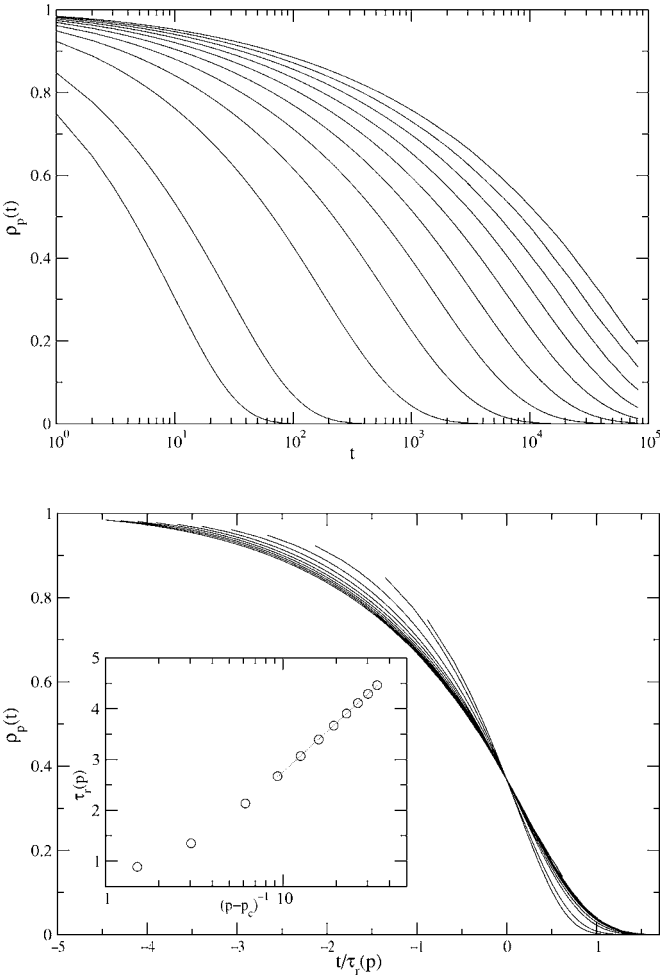

FIG. 12. (a) The relaxation of the persistence spin density $\rho_p(t)$ vs time t for various values of p. (b) A scaling attempt of time string-density superposition on $\rho_p(t)$ with respect to the characteristic relaxation time scale $\tau_r(p)$, where we find a strong violation of the scaling due to the p dependence of the stretching exponent β. The inset shows $\tau_r(p)$ vs $(p-p_c)^{-1}$ which exhibits a power law divergence of $\tau_r(p) \sim (p-p_c)^{-\gamma}$ with $p_c \simeq 0.004$ and $\gamma \simeq 3.23$.

almost the same for $p \leqslant 1/9$. But the exponent β shows some dependence on p: it becomes smaller as p is reduced. Because of this p dependence of the exponent β, the time string-density superposition for $\rho_p(t)$ is violated as demonstrated in Fig. 12(b).

Figure 13 shows snapshots of configurations of persistent spins at different times for $p=1/18$. The dark regions represent the persistent spins. The white regions represent spins at least once flipped. As this figure vividly shows, the way that the active regions penetrate and grow into inactive regions is spatially heterogeneous. This kinetic heterogeneity is perhaps the underlying reason for the p-dependence of the exponent β. We have looked at the p dependence of the relaxation time $\tau_r(p)$ which for convenience is defined as $\rho_p[t=\tau_r(p)]=e^{-1}$. We have obtained the data for smaller p up to $p=1/30$. The relaxation time $\tau_r(p)$ increases rapidly with smaller p. We observed a small but clearly discernable curvature in the increase of $\tau_r(p)$ for small $p \leqslant 1/9$. This may indicate a power law divergence of the relaxation time at a

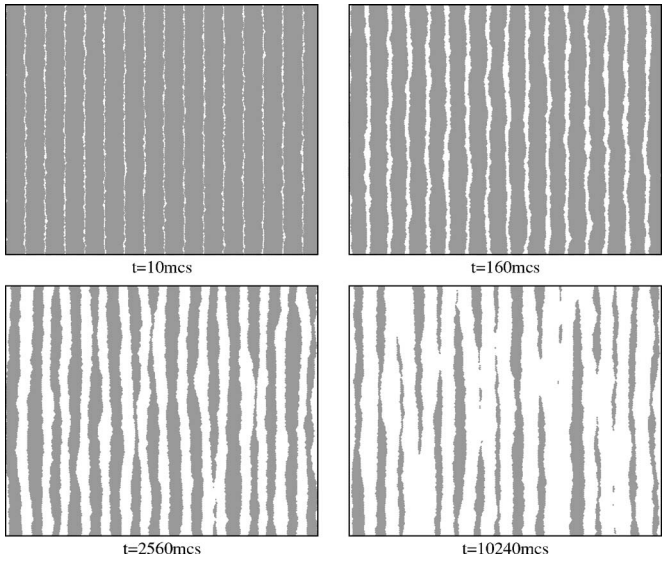

FIG. 13. Snapshots of configurations of persistent spins at different times for $p=1/18$. Dark regions represent the persistent spins, while white regions represent spins which were flipped at least once.

nonvanishing string density p_c, i.e., $\tau_r(p) \sim (p-p_c)^{-\gamma}$. We have tested this interesting possibility in the inset of Fig. 12(b) and we find $p_c \simeq 0.004$ gives a good straight line in a double-log plot of τ_r versus $(p-p_c)^{-1}$ with the exponent $\gamma \simeq 3.23$. The slow relaxation exhibited by the persistent spin density is reminiscent of that found in glassy models.

IV. SUMMARY AND CONCLUDING REMARKS

The string picture obtained from a dimer covering in the dual lattice enables one to classify the macroscopically degenerate ground states into sectors each of which has a unique value of the string number density p. The dominant sector is the one with $p=2/3$, which has the maximum number of ground states. Other sectors are called the minor sectors. The kinetics is nonergodic in the sense that the time evolution within the ground state manifold is confined to the very sector to which the initial configuration belongs, due to the string number conservation. Within each sector the dynamics appears to be ergodic: the nonequilibrium initial state evolves toward the (restricted) equilibrium state. Therefore the kinetics exhibits initial state dependence. If the system is quenched to the zero-temperature from an initial state "outside" the ground state manifold (a typical example is the random disordered initial state), the minor sectors will never be reached. The system always evolves toward the dominant sector. In order to reach the minor sectors the initial state should be one of the corresponding ground states. The situation is somewhat analogous to the nonequilibrium kinetics observed in the spherical p-spin model [31]. In this model, starting from the random initial state the system always evolves toward the highest TAP states [32], and cannot penetrate into the lower TAP states. In order to probe the dynamics within the TAP states [33] one has to start with one of the TAP states.

In this work, we have attempted to characterize the nonequilibrium kinetics observed within the minor sectors with $p<2/3$ of the ground state ensemble of the triangular AFI model. The time evolution proceeds via flips of loose spins only. As the string density is reduced, the number of loose spins becomes smaller. At the same time the zero-loose-spin domain becomes correspondingly larger. In addition, it is anticipated that there will be some cooperative effects present in the dynamics of loose spins. As the string density is reduced from $p=2/3$, we observe an anisotropy in the equilibrium spatial correlation function reflecting the anisotropic fluctuations of the strings and mutual repulsion of the strings. This is in sharp contrast to the case of the dominant sector of $p=2/3$ where all the equilibrium correlations along the three major axes are the same (isotropic). In the case of minor sectors ($p<2/3$), the equilibrium spin correlation function along the vertical direction starts to develop a critical relaxation at short distances, and crosses over to the late-stage critical relaxation at long distances. This early-stage critical region becomes larger as the string density is further reduced, with the crossover length scale exhibiting a divergence of $\xi_{e,V}\sim p^{-2}$. While on the other hand, along the horizontal direction, the length scale is characterized by the typical separation between strings as $\xi_{e,H}\sim p^{-1}$. Therefore in typical simulations the early-stage critical relaxation becomes practically dominant for small enough p (for example $p=1/18$ in the present simulation), pushing the late-stage critical relaxation outside the simulation window.

The equilibrium spin correlation functions for different minor sectors exhibit a scaling behavior when the distance is rescaled with respect to the size of the early-stage critial relaxation region. The same phenomenon of the appearance and growth of the early-stage critical relaxation and crossover to the late-stage critical relaxation manifests in temporal relaxation of the spin autocorrelation function as well. The time duration over which the early-stage critical relaxation is observed tends to diverge algebraically with vanishing string density. In the limit of low string density, the scaling behavior in the nonequilibrium relaxation (fluctuation) dynamics of the system can be simply explained in terms of random walk nature of the strings within the length scale of average separation between neighboring strings. In this regard, we may also remark that the system, at equilibrium in the limit of low string density, could be mapped onto the exactly solvable model system of quantum $(1+1)$-dimensional gas of hard core bosons with repulsive delta function potential of infinite strength [34]. The persistence property exhibits a nonequilibrium glassy relaxation with typical relaxation diverging at a small nonvanishing string density.

We emphasize that in the present work we have focused only on the case of unit winding number for the strings. In a more general case of nonzero slope sectors, further work is needed to identify properties of the nonequilibrium relaxation dyamics within a given ground-state sector.

ACKNOWLEDGMENTS

We thank Professor Jin Min Kim and Dr. Seung-Yeon Kim for useful discussions. This work was supported by Grant R01-2003-000-11595-0 from the Basic Research Program of the Korea Science and Engineering Foundation.

[1] R. Liebmann, *Statistical Physics of Periodically Frustrated Ising Systems*, *Springer Lecture Notes on Physics* No. 251 (Springer, New York, 1986).
[2] G. H. Wannier, Phys. Rev. **79**, 357 (1950); Phys. Rev. B **7**, 5017 (1973).
[3] R. M. F. Houtappel, Physica (Amsterdam) **16**, 425 (1950).
[4] J. Stephenson, J. Math. Phys. **11**, 413 (1970).
[5] J. L. Jacobsen and H. C. Fogedby, Physica A **246**, 563 (1997).
[6] H. W. J. Blöte and M. P. Nightingale, Phys. Rev. B **47**, 15046 (1993).
[7] O. Nagai, S. Miyashita, and T. Horiguchi, Phys. Rev. B **47**, 202 (1993).
[8] C. Zeng and C. L. Henley, Phys. Rev. B **55**, 14935 (1997).
[9] Z.-Y. Chen and M. Kardar, J. Phys. C **19**, 6825 (1986).
[10] L. Gu, B. Chakraborty, P. L. Garrido, M. Phani, and J. L. Lebowitz, Phys. Rev. B **53**, 11985 (1996).
[11] B. Chakraborty, L. Gu, and H. Yin, J. Phys.: Condens. Matter **12**, 6487 (2000); H. Yin and B. Chakraborty, Phys. Rev. E **65**, 036119 (2002).
[12] H. Yin and B. Chakraborty, Phys. Rev. Lett. **86**, 2058 (2001).
[13] A. Dhar, P. Chaudhuri, and C. Dasgupta, Phys. Rev. B **61**, 6227 (2000).
[14] A. N. Berker and L. P. Kadanoff, J. Phys. A **13**, L259 (1980).
[15] P. Hoever, W. F. Wolff, and J. Zittartz, Z. Phys. B: Condens. Matter **41**, 43 (1981).
[16] Z. Rácz and T. Vicsek, Phys. Rev. B **27**, 2992 (1983).
[17] H. W. J. Blöte and H. J. Hilhorst, J. Phys. A **15**, L631 (1982); B. Nienhuis, H. J. Hilhorst, and H. W. J. Blöte, *ibid.* **17**, 3559 (1984).
[18] E. Kim, B. Kim, and S. J. Lee, Phys. Rev. E **68**, 066127 (2003).
[19] D. P. Landau, Phys. Rev. B **27**, 5604 (1983).
[20] G. Forgacs, Phys. Rev. B **22**, 4473 (1980).
[21] C. Moore, M. G. Nordahl, N. Minar, and C. R. Shalizi, Phys. Rev. E **60**, 5344 (1999).
[22] B. Yurke, A. N. Pargellis, T. Kovacs, and D. A. Huse, Phys. Rev. E **47**, 1525 (1993).
[23] F. Rojas and A. D. Rutenberg, Phys. Rev. E **60**, 212 (1999), and references therein.
[24] A. J. Bray, A. J. Briant, and D. K. Jervis, Phys. Rev. Lett. **84**, 1503 (2000).
[25] A. J. Bray, Phys. Rev. E **62**, 103 (2000).
[26] M. V. Mostovoy, D. I. Khomskii, J. Knoester, and N. V. Prokefev, Phys. Rev. Lett. **90**, 147203 (2003).
[27] J. Villain, D. R. Grempel, and J. Lapujoulade, J. Phys. F: Met. Phys. **15**, 809 (1985).
[28] B. Derrida, V. Hakim, and V. Pasquier, Phys. Rev. Lett. **75**, 751 (1995).

[29] A. J. Bray, B. Derrida, and C. Godrèche, Europhys. Lett. **27**, 175 (1994); D. Stauffer, J. Phys. A **27**, 5029 (1994); S. N. Majumdar and C. Sire, Phys. Rev. Lett. **77**, 1420 (1996).
[30] S. Jain and H. Flynn, J. Phys. A **33**, 8383 (2000).
[31] A. Barrat, e-print cond-mat/9701031, and references therein.
[32] L. F. Cugliandolo and J. Kurchan, Phys. Rev. Lett. **71**, 173 (1993).
[33] A. Barrat, R. Burioni, and M. Mézard, J. Phys. A **29**, L81 (1996).
[34] M. Girardeau, J. Math. Phys. **1**, 516 (1960).